American Fern Journal 111(2):86–109 (2021)
Published on 7 June 2021

Microscopic and Metagenomic Evidence for Eukaryotic Microorganisms Associated with Atacama Desert Populations of Giant *Equisetum*

Anchittha Satjarak
Plants of Thailand Research Unit, Department of Botany, Faculty of Science, Chulalongkorn University, Bangkok, Thailand 10330, email: anchittha.s@chula.ac.th

Michael J. Piotrowski
Department of Botany, University of Wisconsin, Madison, WI 53706, USA, email: mpiotrowski5575@gmail.com

Linda E. Graham*
Department of Botany, University of Wisconsin, Madison, WI 53706, USA, email: lkgraham@wisc.edu

Marie T. Trest
Department of Botany, University of Wisconsin, Madison, WI 53706, USA, email: mttrest@wisc.edu

Lee W. Wilcox
Department of Botany, University of Wisconsin, Madison, WI 53706, USA, email: lwwilcox@wisc.edu

Jennifer J. Knack
Department of Biology, University of Minnesota, Duluth, MN 55812, USA, email: jennack3315@gmail.com

Martha E. Cook
School of Biological Sciences, Illinois State University, Normal IL 61790, USA, email: mecook1@lstu.edu

Patricia Arancibia-Avila
Department of Basic Sciences, University of Bío-Bío, Chillan, Chile, email: parancib@ubiobio.cl

Abstract.—Understanding features that fostered the persistence of *Equisetum*–Earth's oldest extant vascular plant genus–since Mesozoic times and through episodes of significant global environmental change, is of current interest in view of modern challenges to plant survival. In addition to known structural and physiological adaptations, we hypothesized that microscopy and shotgun metagenomic sequencing might reveal eukaryotic microorganisms such as fungi that may aid *Equisetum* survival. Here, we report evidence for several lineages of eukaryotic microbes associated with giant *Equisetum xylochaetum*, which dominates vegetation in saline streambeds of remote valleys in the hyper-arid Atacama Desert, Chile. Plant material was collected and field-preserved at two comparatively low-disturbance sites; DNA extracted in Chile using low-shear methods was later sequenced, 18S and 28S rDNA taxonomic marker sequences were selected for SILVAngs classification, allowing comparisons to eukaryotic microorganisms previously inferred for earlier-diverging plant lineages. SEM, fluorescence microscopy, and/or LM of toluidine blue-stained sections of roots indicated protists, epiphytic and endophytic fungi, and cortical nematodes. Eukaryotic genera inferred from 18S rDNA at >100X mean sequencing depth included the ciliate *Engelmanniella*, hyphal chytrid *Monoblepharella*, predatory ascomycete

* corresponding author

Cephaliophora, a salpingoecid choanoflagellate, and an annelid worm. 23S rDNA sequences indicated ascomycete Capnodiales fungi at one site and four types of Pezizomycotina fungi at the other. No evidence for vesicular-arbuscular mycorrhizal fungi was found, but we hypothesized that *Equisetum* may benefit from other types of fungal associations, some possibly inherited from ancestral plant lineages.

KEY WORDS.—horsetails, metagenomic sequencing, scouring rushes, seedless plant microbiomes

The globally widespread genus *Equisetum,* commonly known as "horsetail" or "scouring rush," has been described as the world's oldest and most successful vascular plant genus (Rothwell, 1996). *Equisteum* is the only modern representative of a once-diverse clade of equisetophytes (Class Equisetopsida or Sphenopsida) that originated in the Upper Devonian; the history of genus *Equisetum* extends back to the Mesozoic, indicated by definitive fossil remains of Late Jurassic age (Channing *et al.*, 2011), and possibly the Lower/Middle Triassic (~230 Ma) (Gould, 1968) or even earlier (White, 1894). These dates are consistent with molecular diversification ("timetree" or "molecular clock") analyses indicating a stem age for *Equisetum* of 304.2 Ma (later Carboniferous) (Laenen *et al.*, 2014), and a crown age of 203 Ma (earliest Jurassic) (Clark, Puttick, and Donoghue, 2019). *Equisetum* crown age was estimated at mid-Mesozoic in an analysis that included molecular and fossil data (Elgorriaga *et al.*, 2018).

Structural features shared with the tree-sized (30 m tall) Carboniferous hydrophyte genus *Calamites* (Gifford and Foster, 1989) have been proposed to explain the persistence of genus *Equisetum* over such long geological time periods, and in diverse modern locales (Rothwell, 1996): determinate aerial shoots; production of aerenchyma that fosters growth even in anoxic waterlogged soils; and a persistent, branched, fire- and drought-resistant subterranean rhizome, which produces elongate roots able to access deep water and minerals even when the soil surface is dry. Modern *Equisetum*, which differs from other modern ferns and lycophytes in having a distinctive type of vascular system (Nopun *et al.* 2016), is said to differ structurally from *Calamites* mainly in the absence of secondary xylem (Rothwell and Ash, 2015). Among the modern *Equisetum* species, *E. xylochaetum* Mett., related to, but recently segregated from *E. giganteum* L. (Christenhusz *et al.*, 2019), which forms lush glades in streambeds in Atacama Desert valleys of southern Peru and northern Chile, most closely approaches ancient *Calamites* in size, having stems up to 4.0 cm diameter that reach more than 4 meters in height (Husby, 2013). Experimental field studies have demonstrated that *Equisetum xylochaetum* possesses several physiological adaptations to high salinity conditions associated with arid environment: sodium exclusion and a high degree of homeostasis in stomatal conductance, photosynthesis, and root function over a broad range of groundwater salinities (Husby *et al.*, 2011; 2014). An ancient whole genome duplication (WGD) event was proposed to have helped *Equisetum* to survive the dramatic K-Pg extinction event (Vanneste *et al.*,

2015). Later studies have indicated the occurrence of Carboniferous and Triassic WGD events in the stem lineage, prior to the divergence of modern *Equisetum* beginning in the early Jurassic, raising questions about the role of WGD in long-term lineage survival of Equisetaceae (Clark, Puttick, and Donoghue, 2019).

We hypothesized that in addition to structural, physiological, and possible genomic features, microorganisms might also contribute to *Equisetum* survival under modern stressful conditions such as the hyperarid Atacama Desert, and may also have aided equisetophyte persistence in the remote past. Microorganisms can be transmitted between plant generations and plant microbiomes display evidence of inheritance/evolutionary impacts (*e.g.*, Gehring *et al.*, 2017; Fitzpatrick *et al.* 2018; Walters *et al.* 2018; Yeoh *et al.* 2017). Genetically-determined plant secretions are known to play important roles in establishing and mediating microbiome composition (*e.g.*, Stringlis *et al.*, 2018), indicating a mechanistic explanation for inheritance effects. These findings suggest the possibility that modern *Equisetum* might have inherited the capacity to acquire beneficial microorganisms from ancestral plant populations.

A deep-time perspective of Atacama Desert *Equisetum* microbial associations can be justified by spore evidence for presence of terrestrial plants in northern Chile (Zorritas Formation, Antofagasta Region) since the early Carboniferous (Rubinstein, Petus, and Niemeyer, 2017) and >150 million years of regional geographic stability. Northern Chile has remained at approximately the same latitude since the Late Jurassic (Hartley *et al.*, 2005; Clarke, 2006; Placzek *et al.*, 2014), with relatively moist climate indicated for much of this time and present extreme aridity ensuing in the Holocene (Arroyo *et al.*, 1988). Analysis of organic carbon along aridity gradients in this region has indicated that plant life was likely present in the past in regions that today lack conspicuous vegetation (Knief *et al.*, 2020).

Excepting El Niño-associated rain events (Chávez *et al.*, 2019; Ortega *et al.*, 2019), annual rainfall in the northern Chilean coastal cities of Arica and Iquique is typically 0.5-0.6 mm, the result of subtropical high pressure, cold offshore current, and wind. Very low rates of erosion over long time periods have led to accumulation of usual salts (perchlorates, iodates, and nitrates) in addition to halite and gypsum (Knief *et al.*, 2020; Voight *et al.*, 2020), conditions that also challenge plant growth. Given these extreme environmental conditions, modern Atacama Desert vegetation is sparse; the region has been used as an analog of Mars conditions (*e.g.*, Azua-Bustos *et al.*, 2019). We hypothesized that comparing eukaryotic microorganisms associated with Atacama Desert *Equisetum* with microorganisms previously inferred by similar methods for modern representatives of earlier-diverging plant lineages (Knack *et al.*, 2015; Graham *et al.*, 2017) might indicate microbiome features associated with long-term lineage survival (Graham *et al.*, 2018).

However, at present, the suite of eukaryotic microorganisms associated with *Equisetum* in general, and *E. xylochaetum* in particular, is not well understood. For example, some authorities note that *Equisetum* generally lacks mycorrhizae that would foster nutrient acquisition (Read *et al.*, 2000), but

other studies have provided evidence from microscopy that some species of *Equisetum* harbor vesicular-arbuscular mycorrhizae (VAM) and other fungal associates (Dhilion, 1993; Hodson *et al.*, 2009; Koske *et al.*, 1985). Imaging and metagenomic sequence data have revealed that liverworts and mosses can associate with diverse eukaryotic microbes, including fungi (Knack *et al.*, 2015; Graham *et al.*, 2017). To look for evidence of fungal associations, compare eukaryotic microorganisms among seedless plant lineages, and generally improve knowledge of plant-associated microorganisms, particularly in stressful environments, we employed several microscopy approaches and taxonomic marker genes derived from shotgun metagenomics to survey eukaryotic microorganisms associated with *E. xylochaetum* populations sampled from relatively undisturbed locales in the Atacama Desert, Chile.

Materials and Methods

Source of plant material.—In January 2016, replicate samples of *Equisetum* plants having distinctive stem height and diameter consistent with those described for giant *E. xylochaetum* (Christenhusz *et al.*. 2019) were taken from upper and lower aerial shoots, and rhizomes and/or roots. Plant collections were made from public lands at two sites in the Chilean Atacama Desert by four of the authors (LG, JK, MT, PA-A) for microscopic and metagenomic study. These plant materials were sampled from saline streambeds in deep quebradas (canyons) that occur in the northern part of the Central Depression (Valle Central). The hyper-arid Central Depression lies east of a coastal range of Mesozoic igneous and sedimentary rocks known as the Cordillera de la Costa (Oligocene-Pliocene sediments) and west of the Precordillera (Mesozoic to Eocene) pre-Andean basins of Miocene to Holocene sediments west of the Andes. The collection sites had been employed previously for physiological studies of the same species of *Equisetum* by Husby *et al.* (2011; 2014), who reported some environmental metadata. Soil features, including soil bacterial abundance and diversity, have been reported in some detail for a nearby area of the Atacama (Knief *et al.*, 2020). Geo-reference and other site information related to the current report are provided in Appendix 1.

Plant collectors visited five of the same Atacama locales described by Husby *et al.*, (2011), judging that the two sites for which data are reported here–Huasquiña (also spelled Guasquiña) (HUA) and Chiza (CHI) (names referencing nearby villages)–were the least-disturbed by human activities. These locales are mapped in Husby *et al.*, (2011). In 2016, the particularly remote HUA locale seemed the least-disturbed; although ancient remains of agricultural terraces were present, modern human agriculture was not practiced near the sampled area. The CHI collection site was located approximately 100 meters from Chile Highway 5, but agricultural fields were not observed in the near vicinity. High water tables (0.5 m or less) were previously described for these two locales (Husby *et al.*, 2011), but during our 2016 excavations up to a 1-meter depth, we did not encounter groundwater at

these sites, only moist soil, possibly reflecting annual or seasonal climate variability.

Collectors used new nitrile gloves and implements to reduce the potential for sample contamination. Three technical replicates each from upper and lower stems, rhizomes, and roots, plus one sample of internal tissue at a joint, were represented in collections from HUA from which DNA was subsequently sequenced. By contrast, CHI collections sampled for DNA sequencing included three technical replicates each of upper and lower stems and roots, because rhizomes were not encountered during excavation to a 1-meter depth. We note that underground rhizomes and roots of *Equisetum* are structurally-distinctive (Gifford and Foster, 1989) and therefore easily distinguished from those of co-occurring angiosperms. Although *E. xylochaetum* collections were made from both sites as voucher specimens, the brittle materials were fragmented by compression during transport, so were not appropriate for formal herbarium archiving; these fragmented specimens were stored in author P. A.-A.'s lab at the University of Bio-Bio, Chillan, Chile.

Imaging.—Preliminary microscopic examinations of fresh materials were conducted in the field using a Zeiss Primo Star compound microscope equipped with sub-stage illumination and adaptors for international current (B&H Photo Video, NY, NY). This microscopic examination helped to ensure that plant samples were as free as possible from soil or other loosely-adherent materials. To enable further microscopic imaging after transport to the US, representative plant samples were fixed immediately after collection in 2% glutaraldehyde that was freshly prepared in the field from 70% EM-grade glutaraldehyde (Ted Pella, Inc. Redding, CA, USA). To prepare fresh glutaraldehyde solution just prior to use, 6.8 ml of 0.1M pH 7 phosphate buffer was used to dilute 0.2 ml of 70% glutaraldehyde that had been stored free of air in a 5ml syringe, which was wrapped with Parafilm and double-bagged in plastic to retard leakage or air entry during transport. Fixed plant materials were washed three times in phosphate buffer prior to transport in phosphate buffer; USDA APHIS determined that such materials were not under jurisdiction. No living materials were transported from Chile.

Glutaraldehyde-fixed/buffer-washed roots sampled from CHI were first hand-sectioned for light microscopic examination. Because structures large enough to be eukaryotes were observed within roots, other root samples were further processed for light microscopy and for SEM. Some hand-sections were viewed with use of a Zeiss Axioplan epifluorescence microscope equipped with UV filter G365 FT395 LP420 for assessment of Calcofluor White staining specific for chitin (or cellulose). For microtome-sectioning, a glutaraldehyde-fixed root was dehydrated in an ethanol series, then embedded in LR White resin, hard grade (Ted Pella, Inc., Redding, CA). Following polymerization at 50°C, sections of ~250 nm-thickness were cut using an MT2B Sorvall ultramicrotome and a DuPont diamond knife with water-filled boat, and sections were transferred from the water surface to glass slides using a hand-made wire loop, which was cleaned in 95% EtOH after each use. After low-level heating on a hot plate to evaporate water and adhere microtome-cut

sections to slides, an aqueous solution of 1% toluidine blue + 1% sodium borate was used to stain sections for a short time at low heat. Toluidine blue has been recommended for observation of the hyphae of arbuscular mycorrhizal fungi in embedded plant root tissues (Hulse, 2018), has also been employed to study ectomycorrhizae (Ragonezi and Zavattieri, 2018), and is a recognized method for visualizing root-infecting nematodes (Zhang *et al.*, 2017). Stained slides were rinsed with distilled water to remove excess stain, then returned to low heat to dry, after which Permount (Thermo Fisher Scientific, Waltham, MA) was employed to make permanent preparations. Light microscopic images were recorded using a Nikon D300s digital camera and Camera Control Pro software (Nikon, Melville, NY, USA) or an Olympus BX50 compound microscope equipped with Nikon D810 camera.

For SEM, roots that had been glutaraldehyde-fixed and buffer-washed in the field were hand-sectioned with a razor blade before dehydration in an ethanol series, then critical point dried and coated with iridium prior to examination with a Hitachi S-4800 ultra-high-resolution cold cathode field emission SEM operated at 5 kV.

DNA processing.—Plant samples taken aseptically for metagenomic analyses were stored immediately after field collection in 90% ethanol (EtOH) in sterile conical tubes. Sealing screw caps with a strip of Parafilm (Bemis, Inc. Neenah, WI, USA) proved essential to preventing ethanol evaporation during transport. After 4-8 days of transport in the field, samples for DNA extraction were further processed. Samples were carefully washed to remove EtOH, soil, and any other loosely-associated materials by swirling in three changes of sterile water in sterile petri dishes, before transfer to bead beater tubes. No conspicuous parts of other plants were observed. To improve the proportion of microbial DNA to host plant DNA and to reduce DNA shearing, we did not employ grinding. The goal of reducing shearing was to obtain longer segments of native DNA to reduce the likelihood of artifact sequence formation during downstream contig assembly. These processing methods mirrored those we had earlier used to prepare field-sampled species representing earlier-diverging seedless plant lineages in our previous metagenomic studies (Knack *et al.*, 2015; Graham *et al.*, 2017). For the current study of *E. xylochaetum*, we deliberately employed similar cleaning, sequencing, and analytic methods to facilitate between-lineage comparisons.

To reduce the potential for introduction of exogenous microbes, transfers of plant materials were accomplished using forceps that were dipped into 95% EtOH and then flamed, by operators using new nitrile gloves. DNA extraction was done using the MoBio PowerSoil kit (Qiagen, Hilden, Germany) employing a modified lysis procedure designed to reduce DNA shearing, as suggested by Qiagen technical personnel: samples were vortexed for only a few seconds prior to heating at 70°C for 5 min, a process that was then repeated. Extracted DNA was transported to the US in freezer tubes at ambient temperature, a procedure determined by USDA APHIS not to be under jurisdiction, then kept frozen at -80° F for a few days prior to delivery to the University of Wisconsin-Madison Biotechnology Center for quantification and

sequencing. DNA quantification data indicated that 13 samples obtained from site HUA should be pooled, as were 9 samples from locale CHI. DNA quantities for individual technical replicates were insufficient for finer scale partitioning among plant parts. More than 52 Gb of shotgun metagenomic sequence was obtained using the Illumina HiSeq 2500 platform.

Bioinformatic processing.—Raw reads were trimmed using Trimmomatic version 0.39 (Bolger, Lohse, and Usadel, 2014). MEGAHIT version 1.2.6, designed for handling large, complex metagenomics data sets (Li *et al*. 2015), was employed for assembling contigs from raw sequences. The assembler used paired reads to detect and resolve chimeric contigs produced from misassembly (Ayling, Clark, and Leggett, 2020). Assembly statistics and chimera detection information are provided in Appendix 2. The SILVAngs 1.3 portal was employed to classify contigs containing 18S rDNA and 28S rDNA sequences because eukaryotic microbes are particularly well-represented in the reference databases (Quast *et al*., 2013), and because this classifier had been employed in our earlier metagenomic analyses of eukaryotic microbes associated with seedless plants (Knack *et al*., 2015; Graham *et al*., 2017). UCHIME (ver. 4.2.40; Edgar *et al*. 2011), implemented in Geneious version 9.1.3 (https://www.geneious.com) was used to filter out chimeric contigs (see Appendix 2). Contigs containing annotated 18S rDNA and 28S rDNA sequences were compared against the SSU and LSU SILVA database (Quast *et al*., 2013) using default parameters: minimum score to report chimera = 0.3, minimum divergence ratio = 0.5, weight of a no vote = 8, pseudo-count prior on number of no votes = 1.4, weight of an abstain vote = 1, number of chunks to extract from the query sequence when searching for parents = 4, minimum length of a chunk = 64 bp, maximum number of candidate parents to consider = 2, minimum unaligned sequence length = 10, maximum unaligned sequence length = 10,000, the length of id smoothing window = 32, global alignment.

Contigs were taxonomically processed using the SILVA incremental aligner (SINA SINA version 1.2.10 for ARB SVN, revision 21008; Pruesse, Peplies, and Glöckner, 2012) applied against the SILVA small subunit (SSU) and large subunit (LSU) rRNA SEED and quality controlled (Quast *et al*., 2013). Reads shorter than 50 aligned bases and those with 12% ambiguities or homopolymers were excluded before further processing, as were likely contaminants and artifacts and those having low alignment quality scores. Identical reads were identified and unique reads clustered using cd-hit-est software (ver. 3.1.2; Li and Godzik, 2006) running in accurate mode, ignoring overhangs, and applying identity criteria of 1.00 and 0.98 as operational taxonomic units (OTUs) for classification performed by local nucleotide BLAST search against the non-redundant version of the SILVA SSU and LSU reference data sets (release 132), using blastn, version 2.2.30+, with standard settings (Camacho *et al*., 2009). Classification of each OTU reference read was mapped onto all reads assigned to the respective OTU. Reads for which there were no or weak (% sequence identity + % alignment coverage)/2 = <93) BLAST hits remained unclassified and were labeled "no relative" in SILVAngs fingerprint and Krona charts (Ondov, Bergman, and Phillippy, 2011). These

methods were initially used by Klindworth *et al.*, (2013) and Ionescu *et al.*, (2012). The above paragraph has been paraphrased from SILVAngs project reports, as recommended in those reports. Quality and settings information can be found in Appendix 3.

Genomic coverage was estimated for most of the classified eukaryotic taxa as a means of gaining some insight into relative abundance. Because the sequence data were obtained by shotgun metagenomic methods, amplification bias was not an issue, as can be the case when input sequences are amplicons. However, we note that for eukaryotes, sequencing depth levels may be influenced by multicellularity or genomic duplication history, and do not represent accurate quantitative assessment of microbial population levels.

For calculation of genomic coverage, trimmed raw reads were aligned to SILVA references using BWA version 0.7.4 non-model species alignment (Li and Durbin, 2009). Mapped reads were filtered and converted to fastq format using SAMtools version 1.7 and BEDtools version 2.26.0 (Quinlan and Hall, 2010). Reads were then mapped to their corresponding SILVA reference sequence using Geneious version 9.1.3 (https://www.geneious.com). Mean and maximum coverage were calculated using the Geneious function ''statistics.'' We employed coverage for the gene region of greatest abundance, indicated by use of the CyVerse Discovery Environment (https://de.cyverse.org/de/). Taxa inferred from 18S or 28S rDNA sequences at a mean coverage level $\geq$10X were considered to have been detected, and were employed for evolutionary comparisons. Taxa inferred at a mean coverage level $\geq$50X were considered relatively abundant. Because assembler pipelines change with time and investigators may have reasons for choosing particular assemblers, to facilitate use by others, we have archived raw, rather than assembled, metagenomic sequence in the NCBI Short Read Archive (http://www.ncbi.nlm.nih.gov/sra) as BioProject PRJNA555713. Sequence data for the HUA site are in accession SAMN12326833, and sequence data for the CHI site are in accession SAMN15794710.

Because this report focuses on eukaryotic microbial associates, *E. xylochaetum*-associated prokaryotic microorganisms and their genes and most sequences related to the host plant genome, which are present in the metagenome, are not described here. However, plastid marker sequences *rbcL*, *rps4*, and *trnL-F*, previously employed to explore species relationships within extant *Equisetum* species (Christenhusz *et al.*, 2019) were extracted from metagenomic data for use in corroborating our identification of the host plant as *E. xylochaetum* based on distinctive structural traits.

Phylogenetic analysis.—Reference *Equisetum* plastid sequences were obtained from GenBank, accessed in July, 2020. *Equisetum bogotense* isolates 40800, 40801, 40802, and 40827 were used as an outgroup cluster, as this species was previously known to represent the earliest-diverging of the modern species (Christenhusz *et al.*, 2019). Nucleotide sequences were aligned using MAFFT v7.402 (Katoh et al. 2013) and the substitution model computed using ModelTest-NG v0.1.5 (Darriba et al. 2020). Maximum likelihood (ML) analysis was performed using RAxML v8.2.12 (Stamatakis 2014) on the XCEDE

Portal for CIPRES (Miller, Pfeiffer, and Schwartz, 2010) using GTR+I+G substitution model. Bayesian analysis were performed with MrBayes v3.2.6 (Ronquist and Huelsenbeck 2003). Four independent chains were run for 100,000 cycles and consensus topologies calculated after 25,000 burn-in cycles.

Results

Microscopy.—LM observations of glutaraldehyde-fixed roots sampled from the Chiza (CHI) site revealed evidence for eukaryote-sized structures on the surfaces of roots and root hairs, and within root cortex cells. Hyaline branched-filaments having diameters <10 μm, which were observed by LM on and within cross-sectioned root cells in which amyloplasts were also visible (Fig. 1a), and which fluoresced blue-white in UV excitation after Calcofluor White staining (and did not display red autofluorescence typical of chlorophyll) (data not shown) were interpreted as fungal hyphae. Thin filaments having similar features present on or within root hairs were also interpreted as fungal hyphae. Septa were sometimes visible in putative hyphae of Calcofluor White-stained material. Darkly-pigmented septate hyphae (commonly known as "dark septate hyphae") were not observed by microscopic examination in the field or lab. Cortical cells of some portions of microtome-sectioned, toluidine blue-stained roots contained larger diameter structures consistent with putative identification as nematodes; such profiles sometimes traversed root cell walls (Fig. 1b). The surfaces of putative nematodes exhibited fine cuticular annulations when viewed at high magnification (Fig. 1c). *Equisetum* root cortical cells that contained nematode-like structures and nearby cells were devoid of cytoplasmic contents such as amyloplasts (Fig. 1b,c).

SEM examination of hand-cut cross sections revealed evidence that microbes of dimensions consistent with classification as prokaryotes and/or eukaryotes were present on outer surfaces of root epidermal cells and contorted root hairs (Fig. 2 a-d). Some of the epimicroorganisms displayed sizes and shapes consistent with unicellular protists (Fig. 2c) and fungi having branched hyphae and specialized cells (Fig. 2d). Higher magnification SEM views revealed the presence of structures consistent with identification as fungal hyphae within root cortical cells, including cells containing rounded structures interpreted as amyloplasts (Fig. 3a). Some of the root cortical cells containing fungal hyphae-like structures lacked structures interpreted as amyloplasts (Fig. 3b). No microscopic evidence for vesicular-arbuscular mycorrhizal fungi was observed for either of the sampled locales.

Sequence-based eukaryotic classifications.—Metagenomic evidence included relatively high coverage of host *Equisetum* 18S rDNA at the lowest-disturbance site, Huasquiña (HUA). Host plant 18S rDNA was likewise confirmed for Chiza (CHI). Phylogenetic analysis employing multiple plastid marker genes indicated that the host plant was *E. xylochaetum* (Fig. 4). At both sites, 18S rDNA sequences were classified as Poales angiosperms: *Juncus* at HUA; *Echinochloa* and *Setaria* at CHI. Eukaryotic taxa whose 18S rDNA

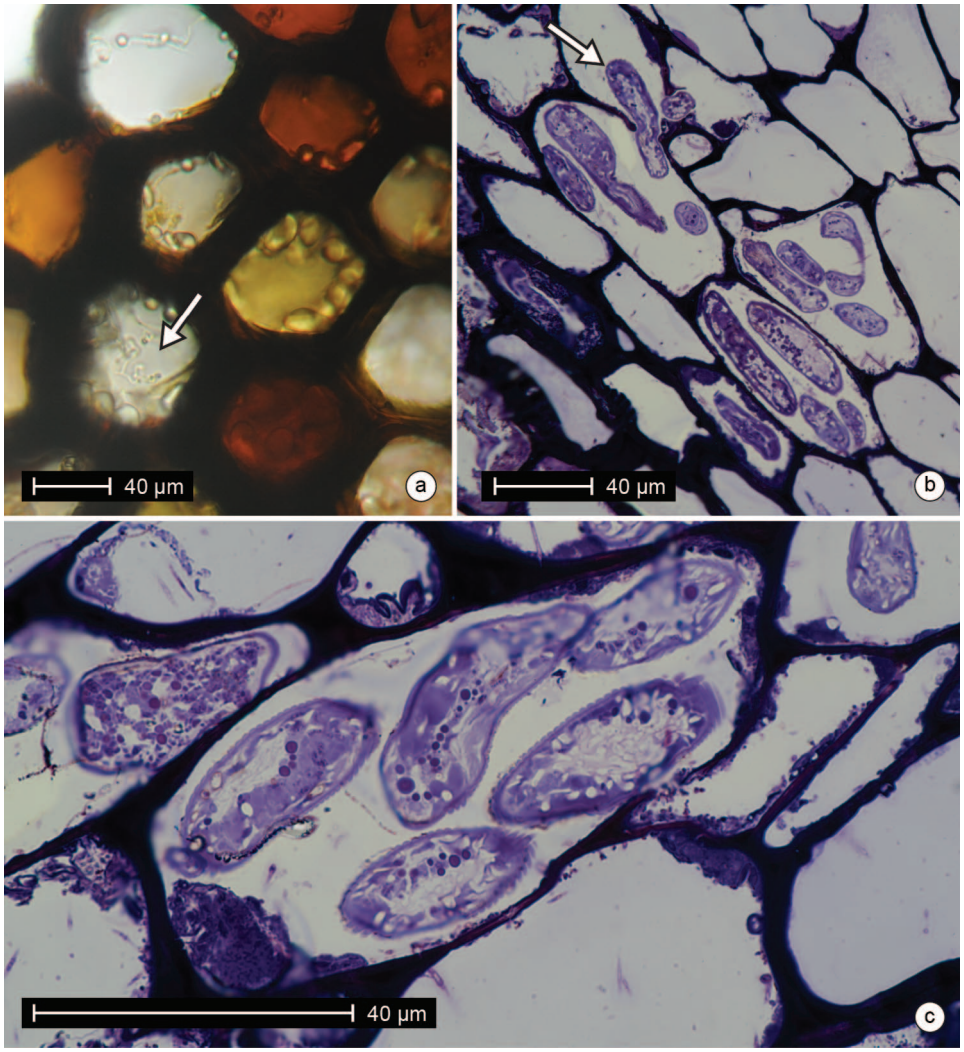

FIG. 1. LIGHT MICROSCOPY. Sections showing eukaryotic microbial associates of *E. xylochaetum* root sampled from the Chiza (CHI) site. **(a)** Hand-cut section showing hyaline branched filaments interpreted as fungal hyphae within root cortical cells (arrow), whose walls are thick and darkly-pigmented. **(b)** Toluidine blue-stained thick section made with microtome and diamond knife. Structures interpreted as profiles of nematodes are located within cortical cells and in apparent transit between cortical cells (arrow). **(c)** Enlarged view of a root cortical cell containing structures interpreted as profiles of nematodes whose surfaces bear fine annulations. Such cortical cells in root regions infected by putative nematodes lack cytoplasmic features such as amyloplasts that occur in un-infected root regions.

sequences were present in mean coverage levels ≥100X at HUA and CHI are summarized with mean and maximum coverage levels in Table 1. At site CHI no eukaryotic taxa were inferred from 18S or 28S rDNA at mean sequencing depths ≥100X, except the host plant *Equisetum* (mean sequencing depth =

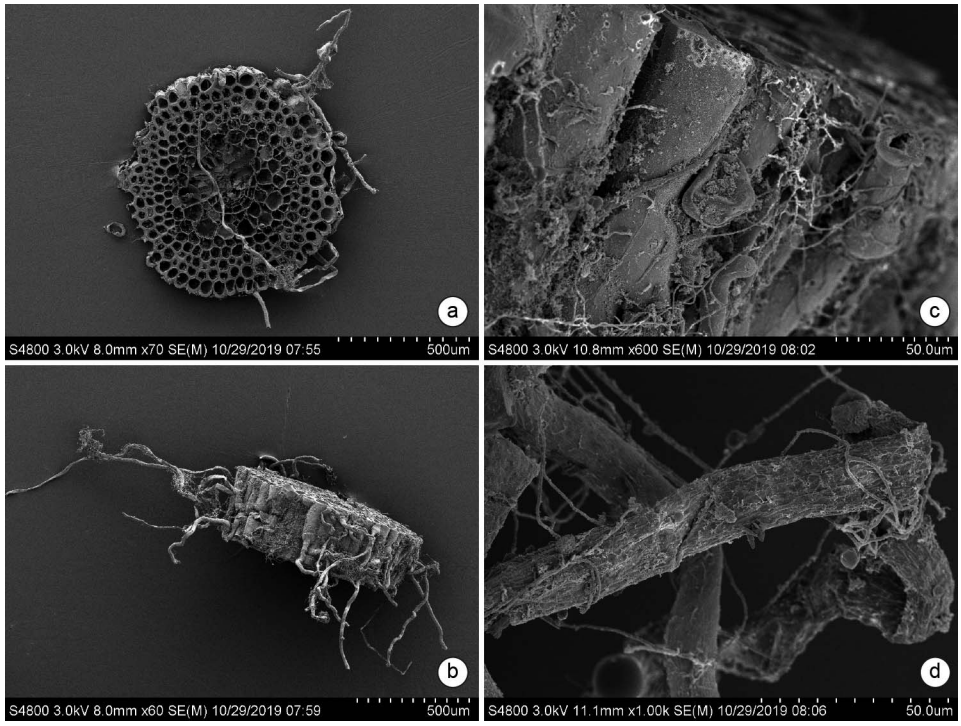

FIG. 2. SCANNING ELECTRON MICROSCOPY. **(a)** Top-view of a hand-cut section of an *E. xylochaetum* root, showing central stele of relatively thin-walled cells, cortex cells having thicker cells, scalloped outer root surface, and emergence of contorted root hairs from root epidermal cells. **(b)** Side-view of the same hand-cut section of an *E. xylochaetum* root showing scalloped root surface and emergence of contorted root hairs from epidermal cells. **(c)** Magnified side-view of root showing an attached biofilm of structures interpreted as eukaryotic and prokaryotic epibionts. The flattened spherical object at center was interpreted as a possible unicellular protist. Narrow threads are of sizes consistent with fungal hyphae and filamentous bacteria. (d) Magnified view of contorted root hairs, showing associated structures interpreted as eukaryotic and prokaryotic microorganisms. A branched filament at the right side was interpreted as fungal hyphae.

1184X, maximum depth = 2420X). 28S rDNA sequences classified as (Pezizomycotina) Capnodiales ascomycete fungi were noted from CHI, but not detected by 18S rDNA.

At site HUA, four types of Pezizomycotina fungi were indicated by 28S rDNA; one of these, classified as Pezizales, had a mean sequence coverage of 146X (maximum 2181X). An HUA Pezizales ascomycete classified as *Cephaliophora* was detected by 18S rDNA signal (212X mean coverage, 1304 maximum coverage). At HUA, 18S rDNA also indicated presence of the chytrid *Monoblepharella* (mean 270X, max 2235X coverage). No sequence evidence for the presence of arbuscular mycorrhizal fungi was found at either site.

At HUA, additional types of microbial eukaryotes were indicated by 18S rDNA sequence data. A salpingoecid choanoflagellate protist was inferred by mean of 291X and maximum 2297X sequence coverage. A haplotaxid annelid

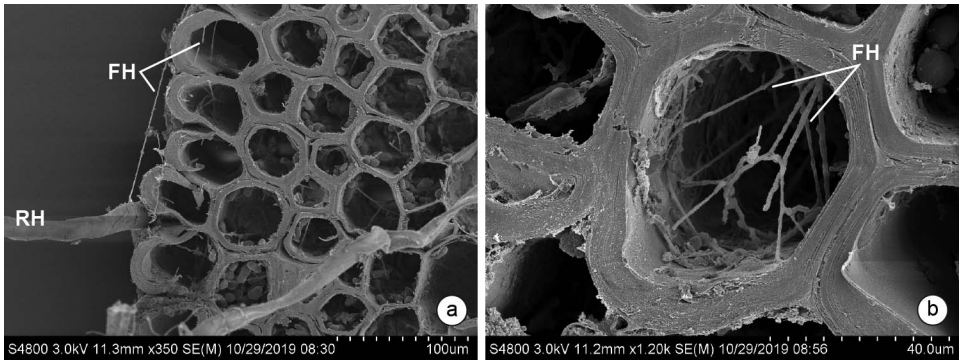

FIG. 3. SCANNING ELECTRON MICROSCOPY. **(a)** A higher magnification view of part of the root section shown in Fig. 2a, showing root hairs (RH) and thin filaments interpreted as epiphytic and endophytic fungal hyphae (FH). Inner cortical cells contain rounded structures interpreted as amyloplasts. No evidence for nematode infection was observed in this root section. **(b)** A root cortical cell containing thin, branching filaments interpreted as fungal hyphae (FH). At this magnification, root cortical cell wall layering is apparent.

microanimal was inferred at mean 121X, maximum 1031X. The unicellular hypotrich ciliate *Engelmanniella* was inferred at a mean 191X, maximum 1397X sequence coverage. A thaumatomonad rhizarian protist was also inferred to occur at HUA in high sequence coverage (mean 136X, maximum 2145X).

Krona analysis of SSU (16S rDNA + 18S rDNA) sequences filtered from the metagenomic data for site HUA indicated that 51% of SSU sequences were not classifiable based on the current content of taxonomic databases, and that bacterial sequences represented a higher proportion of classifiable sequences than did eukaryotic sequences (Fig. 5). Similar Krona analysis for site CHI likewise indicated dominance by bacterial taxa, with 26% of sequences not classifiable on the basis of current taxonomic databases; among eukaryotes, only vascular plants were indicated (analysis not visualized).

DISCUSSION

Overview.—Phylogenetic analysis of multiple plastid marker genes previously employed to study *Equisetum* species diversification (Christenhusz *et al.*, 2019) was consistent with structural information indicating that the host plant was *E. xylochaetum*. Microscopy and molecular data were consistent in indicating the close association of eukaryotic microorganisms, including fungi, with *E. xylochaetum* sampled from two relatively undisturbed Atacama Desert sites. The 28S rDNA marker revealed aspects of eukaryotic diversity not apparent from the 18S rDNA data alone, indicating the value of employing more than one taxonomic marker. Although replicate DNA samples were taken from multiple plant parts, to achieve DNA levels needed for shotgun sequencing, DNA from replicates and

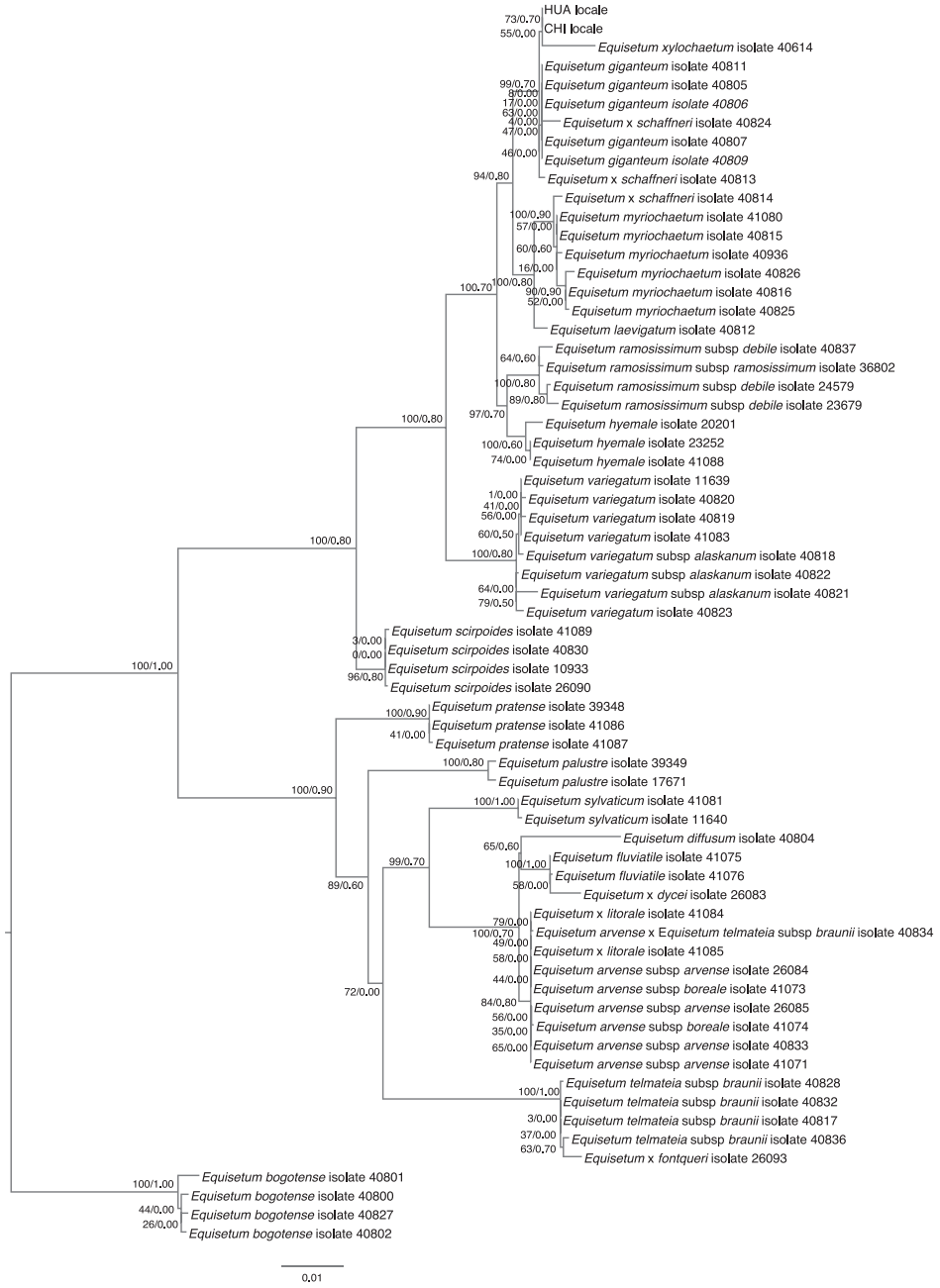

FIG. 4. HOST PHYLOGENETIC RELATIONSHIPS. Phylogenetic relationships of *Equisetum* sampled from the HUA and CHI locales, based on multiple plastid marker genes. Maximum likelihood/Bayesian values indicate that the sampled plants are more closely related to reference *E. xylochaetum* isolate 40614 than to other databased *Equisetum* sequences, a result consistent with distinctive structural features.

TABLE 1. Eukaryotic taxa inferred from 18S rDNA sequence at >100X mean sequencing depth from *Equisetum xylochaetum* sampled at the HUA and CHI sites.

Taxa at HUA	Informal name; phylum	Mean sequencing depth	Maximum sequencing depth
Equisetum	giant horsetail plant; Monilophyta	1021X	2402X
Juncus	rush plant; Anthophyta	1651X	2498X
Engelmanniella	hypotrich ciliate protist; Ciliophora	191X	1397X
Monoblepharella	hyphal chytrid; Chytridiomycota (Spatafora *et al.*, 2016) or Monoblepharomycota (Tedersoo *et al.*, 2018)	270X	2235X
Cephaliophora	Ascomycota	212X	1304X
Salpingoecidae	choanoflagellate protist; Choanoflagellata	391X	2297X
Haplotaxida	haplotaxid worm; Annelida	121X	1031X
Taxa at CHI			
Equisetum	Giant horsetail plant; Monilophyta	1184X	2429X

plant parts had to be pooled, thereby precluding statistical comparisons or efforts to localize microbes on plants. The proportions of sequence contigs that could not be classified based on the information content of current taxonomic databases indicate high potential for future discovery of microorganisms new to science. Comparisons of eukaryotic microbial components of *E. xylochaetum* microbiomes to those inferred in our previous, similarly-conducted metagenomic studies of modern representatives of earlier-diverging, non-vascular plant lineages revealed some commonalities of evolutionary interest.

Locale comparison.—Relatively-abundant 18S rDNA sequence classified as *Equisetum* was obtained for both sampling sites. Sequences indicating co-occurring Juncaceae were likewise consistent with observations of such plants at the sampled locales, though *E. xylochaetum* was judged to dominate the vegetation. Although the sequencing depth of 18S rDNA we report for the host was similar to that of 18S rDNA signal for co-occurring flowering plants (Juncaceae), this is not evidence that the microbiome information obtained in this study might apply to plants other than *E. xylochaetum*. No visible parts of plants other than *E. xylochaetum* were included in microscopically-examined and well-washed samples subjected to DNA sequencing, but it is possible that small amounts of pollen or small seeds from co-occurring angiosperm species might have been attached to surfaces of sequenced *Equisetum*. We had purposefully not employed grinding during DNA extraction, to avoid flooding metagenomic DNA with that from the large host plant, and to reduce DNA shearing, to obtain longer pieces of native DNA to reduce potential impacts of artifact formation during contig assembly. This lack of grinding constrained the sequencing depth of 18S rDNA for the host plant, explaining why the mean sequencing depth inferred for the *E. xylochaetum* host was not noticeably larger than those of sequences indicating co-occurring flowering plants likely represented by microscopic pieces. Despite the advantages of not grinding, it is

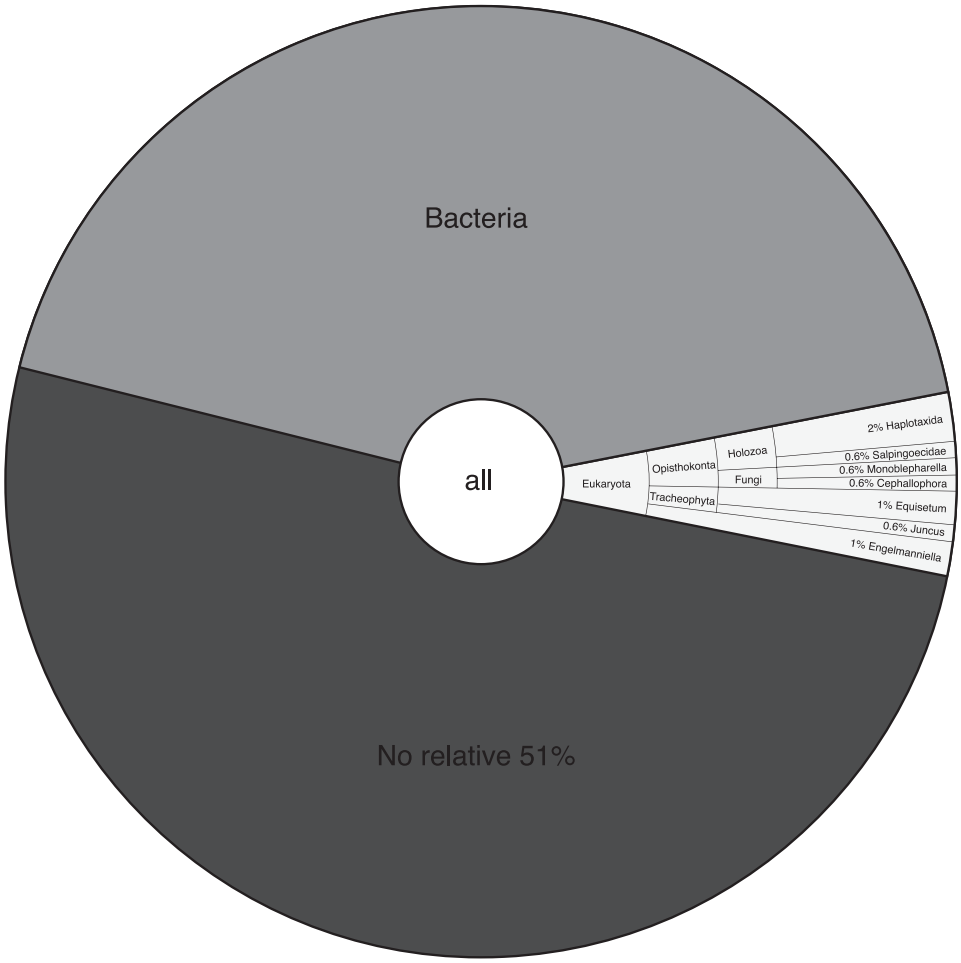

FIG. 5. SILVAngs Krona analysis. Pie chart showing relative proportions of metagenomic contigs classified as Eukaryota, Bacteria, and No Relative. About 6% of sequences classified as the host plant *Equisetum*, a co-occurring angiosperm (*Juncus*), the protist *Engelmanniella*, fungi, or microanimals. The large percentage of sequences not classifiable based on the current content of taxonomic databases suggests high potential for discovery of microorganisms new to science.

possible that grinding might have increased the chances of obtaining DNA sequence for endophytic taxa.

Relatively abundant 18S rDNA evidence at the HUA site for the hypotrich ciliate *Engelmannia* was consistent with relatively abundant HUA 28S rDNA indicating a hypotrich ciliate, but neither marker detected ciliates at CHI. Relatively abundant 28S rDNA also indicated the presence at HUA of a thaumatomonad rhizarian not detected at CHI, and relatively-abundant 18S rDNA indicated presence at HUA but not at CHI of a salpingoecid choanoflagellate–member of a bacterivorous opisthokont lineage closely

related to animal ancestry. Although these observations might suggest that the microorganisms associated with *E. xylochaetum* at the HUA site were richer in protist diversity than at CHI, the difference might have resulted from lack of rhizome samples for CHI.

Sequence evidence from both sites for fungal associates of *E. xylochaetum* was consistent with evidence from microscopy studies of samples from CHI by indicating the likely importance of fungi. Immediate field-processing of samples for later shotgun metagenomic DNA sequencing and microscopy, followed by longer-term freezer storage of extracted DNA and refrigerator storage of glutaraldehyde-fixed/buffer washed samples for microscopy, reduced the potential for later contamination with exogenous fungi. Sequence and microscopy data were consistent in indicating the presence of narrow fungal filaments, but not arbuscular mycorrhizal fungi (AMF), whose hyphae are often relatively wide and may bear distinctive large spores. Because our sampling was necessarily limited in scope, it is theoretically possible that AMF were present, but our collections missed them. If AMF were absent, a number of possible causal factors might be invoked.

Such factors include the typical presence in *Equisetum* tissues of high silica content, which has been hypothesized to retard fungal invasion (Guerriero *et al.*, 2018). *Equisetum* species are also known to produce alkaloids such as nicotine that might influence microbial associations; *E. giganteum* (closely related to *E. xylochaetum*) produces some alkaloids, such as palustridiene, that are not present in all *Equisetum* species (Tipke *et al.*, 2019). Extreme environmental conditions peculiar to the Atacama Desert might also be involved.

Another possible factor is the moist stream-bed environments from which we sampled Atacama *Equisetum*. A meta-analysis of 34 studies of the occurrence of arbuscular mycorrhizal fungi (AMF) in the roots of wetland plants worldwide concluded that though AMF colonization was widespread, the level of colonization was relatively low, particularly in lakes and streams, possibly reflecting locale-specific features (Fusconi and Mucciarelli, 2018). High salinity is an ecological feature that could in theory influence AMF colonization, because high salinity conditions were documented for the particular streambed populations of *E. xylochaetum* (Husby *et al.*, 2011) that we sampled some years later. However, a recent molecular sequence analysis of the effects of salinity on soil microbial communities (in China) indicated that glomalean fungi were present up to the highest level surveyed (>4 grams per kilogram), though species shifts were noted (Zhang *et al.*, 2019). While some evidence for presence of AMF fungi was observed in association with subsurface parts of *Equisetum* sampled from Canadian locales, other types of fungi were considered to be more abundant (Hodson *et al.*, 2009), raising the possibility that *Equisetum* may employ beneficial fungal associates in addition to AMF.

Experimental studies have indicated that ascomycete (*Pezoloma ericae*, Helotiales, Pezizomycotina) associations similar to those of ericoid flowering plants occur in leafy liverworts; radiolabeled phosphorus was used to

demonstrate provision of P by fungi to the plants, and radiolabeled carbon to demonstrate movement of plant photosynthate to fungi (Kowal *et al.*, 2018). Helotiales were among diverse ascomycetes we had earlier inferred from 18S and 28S rDNA sequences (derived from metagenomic data) to associate with the thalloid liverwort *Conocephalum conicum* (Knack *et al.*, 2015). Although Helotiales fungi were not identified using similar methods in our samples of Atacama *E. xylochaetum*, several other Pezizomycotina orders (Pezizales, Glomerellales, Sordiariales, Capnodiales) were inferred. Pezizales includes ectomycorrhizal representatives (Tedersoo *et al.*, 2006; Nouhra *et al.*, 2013). These observations raise the possibility that some of the Pezizomycotina inferred in the current analysis to occur in the eukaryotic microorganisms associated with *E. xylochaetum* might provide similar nutrient provisioning functions that might be explored in future studies.

Atacama Desert populations of *E. xylochaetum* might also benefit by partnering with predatory ascomycete fungi to reduce root nematode infestation. We found abundant sequence evidence (18S rDNA mean sequence depth = 212X, maximum 1304X) for the ascomycete *Cephaliophora*, whose narrow hyphae can produce adhesive pegs that attract rotifers and tardigrades within which hyphae ramify (Barron, Morikawa, and Saikawa, 1990), or wind around nematodes (Tubaki, 1956). Our microscopic evidence for the presence in *Equisetum* roots of nematode-like structures (at the CHI locale) demonstrates that root nematode infestation can be an issue for Atacama Desert *Equisetum* populations. The fossil record suggests that plant parasitic nematodes were present prior to the origin of roots; today several clades of nematodes parasitize parts of diverse vascular plants (Smant, Helder, and Goverse, 2018). Leaf-infecting nematodes are known for ferns and lycophytes (*e.g.*, Wu *et al.*, 2016), though we did not locate any previous reports of nematode attack of *Equisetum* roots. Nematode feeding involves the secretion of plant cell wall-degrading enzymes, possibly explaining cell wall breaches and evidence for cell-to-cell nematode movement we detected in Atacama *E. xylochaetum* roots, using microscopy. Our microscopy-based evidence that nematode-infected *Equisetum* roots are devoid of cellular contents (*e.g.*, amyloplasts) generally present in non-infected roots suggests that nematodes were ingesting root cell contents; we did not observe evidence in *E. xylochaetum* for the formation of root cell syncytia, such as were described from toluidine blue-stained microtome sections of nematode-infected angiosperm roots by Zhang *et al.*, (2017). Given the possibility that *Equisetum*-like plants have occupied northern Chile over geological time periods, including the transition from mesic to xeric environmental conditions, nematode attack might have selected for partnerships involving nematode-feeding ascomycete fungi such as *Cephaliophora*.

Although we detected substantial 18S rDNA sequence evidence for the presence of a haplotaxid annelid at the HUA site, sequences classified as nematodes were not found in our Atacama data. Microscopic examination of multiple sections of roots sampled from CHI suggested that nematodes were

localized, because evidence of these microanimals or their feeding (*e.g.*, cortical cell wall damage, absence of amyloplasts) was not always present. It is likely that by chance, none of the technical replicate samples we employed for sequencing included nematode-infected tissues. Alternatively, our purposeful lack of grinding to reduce host DNA input and increase read length to reduce potential assembly artifact, might also have reduced the chances of finding sequence evidence for nematodes and other types of intracellular eukaryotic microorganisms.

Comparisons to eukaryotic microorganisms associated with representatives of other seedless plant lineages.—Our previous metagenomic and microscopy studies of *Conocephalum conicum* (sampled from rock surfaces to reduce input from soil) and the peat moss *Sphagnum fimbriatum* (sampled from Chilean Patagonia) revealed the presence of diverse types of fungal associates (Knack *et al.,* 2015; Graham *et al.*, 2017), including potentially mutualistic glomaleans (in the case of *C. conicum*) and Mortierellales. Physiological evidence for carbon-for-nitrogen exchange was obtained for a representative lycophyte associated with Mucoromycotina root fungi (Hoysted *et al.*, 2019). Amplicon analyses have indicated the presence of both Mucoromycotina and Glomeromycotina observed to be associated with gametophytes of the ferns *Angiopteris lygodiifolia* and *Osmunda japonica* (Ogura-Tsujita *et al.*, 2019). By contrast, neither of these fungal groups was inferred to be represented among microbial associates of *E. xylochaetum*.

Ascomycete associations seem to be more prevalent in our samples of Atacama *E. xylochaetum*. Molecular evidence for Capnodiales ascomycetes at CHI was a feature shared with both *C. conicum* and *S. fimbriatum*, as were sequences classified as Sordariomycetes at HUA. These commonalities might reflect ancient association traits that could be further explored by characterizing additional seedless plant microbiomes for comparative study. Additional approaches to classification of molecular sequences (*e.g.*, other rDNA sequence regions) could be employed using our archived metagenomic sequence data for these seedless plant species, to potentially gain more definitive fungal classifications, particularly as sequence databases enlarge. Future physiological studies of ascomycete associations with seedless plants may provide clues regarding the functional nature of the *Equisetum*-fungal associations we detected in the Atacama Desert.

Metagenomic evidence for hyphal chytrid (*Monoblepharella*) association with *E. xylochaetum* at HUA, consistent with a report of this genus from South America (Brazil) (Rocha *et al.*, 2015), is of interest because chytrids were also inferred to associate with *C. conicum* (Knack *et al.*, 2015). *Monoblepharella* represents a lineage thought to have evolved hyphae independently of other hyphal fungi, and is thus of evolutionary interest (Powell, 2017), although potential functional aspects of interactions with seedless plants remain to be determined. The metagenomic sequence evidence we found for *E. xylochaetum* association with a ciliate (*Engelmanniella*) at the HUA site recalls sequence evidence for several other ciliate types associated with *S. fimbriatum*; rhizarian protists and a choanoflagellate were also inferred to

associate with both *E. xylochaetum* and the peat moss *S. fimbriatum* (Graham *et al.*, 2017). These protist commonalities may reflect moist habitat conditions and possibly reflect earlier, more mesic conditions likely present in the Atacama region prior to the Holocene onset of aridity (Arroyo *et al.*, 1988; Knief *et al.*, 2020). An emerging deep-time view of the Atacama region is of an ancient mesic, vegetated terrain that might have supported extensive plant populations–including species of *Equisetum*–for long time periods, with such populations gradually becoming restricted to the streambeds of deep valleys as landscape aridity increased. Modern global climate change effects on water supplies might ultimately impact the hardy, persistent *Equisetum xylochaetum* groves of the Atacama Desert.

Acknowledgements

Professor José Delatorre-Herrera (Universidad Arturo Prat, Iquique, Chile) provided key logistical assistance and chemical supplies that were much appreciated. Professor Luis Sobrevia (Pontificia Universidad Católica de Chile, Santiago) kindly provided access to a well-equipped molecular biology laboratory essential for DNA extractions. Computing resources employed for metagenomic sequence analyses were funded by NSF grant DEB-1119944 to L. E. Graham. We thank Sarah Friedrich for generating illustrations.

Literature Cited

Arroyo, M. T. K., F. A. Squeo, J. J. Armesto, and C. Villagran. 1988. Effects of aridity on plant diversity in the northern Chilean Andes: Results of a natural experiment. Annals of the Missouri Botanical Garden 75:55-78.

Ayling, M., M. D. Clark, and R. M. Leggett. 2020. New approaches for metagenome assembly with short reads. Briefings in Bioinformatics 21:584-594.

Azua-Bustos, A., C. Gonzalez-Silva, M. A. Fernandez-Martinez, and C. Arenas-Fajardo. 2019. Aeolian transport of viable microbial life across the Atacama Desert, Chile: Implications for Mars. Scientific Reports 9:11024.

Barron, G. L., C. Morikawa, and M. Saikawa. 1990. New *Cephaliophora* species capturing rotifers and tardigrades. Canadian Journal of Botany 68:685-690.

Bolger, A. M., M. Lohse, and B. Usadel. 2014. Trimmomatic: A flexible trimmer for Illumina sequence data. Bioinformatics 30:2114-2120.

Camacho, C., G. Coulouris, V. Avagyan, N. Ma, J. Papadopoulos, K. Bealer, and T. Madden. 2009. BLAST+: architecture and applications. BMC Bioinformatics 10:421.

Channing, A., A. Zamuner, D. Edwards, and D. Guido. 2011. *Equisetum thermale sp. nov.* (Equisetales) from the Jurassic San Agustín hot spring deposit, Patagonia: Anatomy, paleoecology and inferred paleoecophysiology. American Journal of Botany 98:680-697.

Chávez, R. O., A. Moreira-Muñoz, M. Galleguillos, M. Olea, J. Aguayo, A. Latin, I. Aguilera-Betti, A. A. Muñoz, and H. Manríquez. 2019. GIMMS NDVI time series reveal the extent, duration, and intensity of "blooming desert" events in the hyper-arid Atacama Desert, Northern Chile. International Journal of Applied Earth Observation and Geoinformation 76:193-203.

Christenhusz, M. J. M., L. Bangiolo, M. W. Chase, M. F. Fay, C. Husby, M. Witkus, and J. Viruel. 2019. Phylogenetics, classification and typification of extant horsetails (*Equisetum*, Equisetaceae). Botanical Journal of the Linnaean Society 189:311-352.

Clark, J. W., M. N. Puttick, and P. C. J. Donoghue. 2019. Origin of horsetails and the role of whole-genome duplication in plant macroevolution. Proceedings of the Royal Society B 286:2019.1662.

Clarke, J. D. A. 2006. Antiquity of aridity in the Chilean Atacama Desert. Geomorphology 73:101-114.

Darriba, D., D. Posada, A. M. Kozlov, A. Stamatakis, B. Morel, and T. Flouri. 2020. ModelTest-NG: a new and scalable tool for the selection of DNA and protein evolutionary models. Molecular Biology and Evolution 37:291-294.

Dhilion, S. S. 1993. Vesicular-arbuscular mycorrhizas of *Equisetum* species in Norway and the U.S.A.: occurrence and mycotrophy. Mycological Research 97:656-660.

Edgar, R. C., B. J. Haas, J. C. Clemente, C. Quince, and R. Knight. 2011. UCHIME improves sensitivity and speed of chimera detection. Bioinformatics 27:2194-2200.

Elgorriaga, E., I. H. Escapa, G. W. Rothwell, A. M. F. Tomescu, and N. R. Cuneo. 2018. Origin of *Equisetum*: Evolution of horsetails (Equisetales) within the major euphyllophyte clade Sphenopsida. American Journal of Botany 105:1286-1303.

Fitzpatrick, C. R., J. Copeland, P. W. Wang, D. S. Guttman, P. M. Kotanen, and M. T. J. Johnson. 2018. Assembly and ecological function of the root microbiome across angiosperm plant species. Proceedings of the National Academy of Sciences, U. S. A. 115:E1157-E1165.

Fusconi, A. and M. Mucciarelli. 2018. How important is arbuscular mycorrhizal colonization in wetland and aquatic habitats? Environmental and Experimental Botany 155:128-141.

Gehring, C. A., C. M. Sthultz, L. Flores-Rentería, A. V. Whipple, and T. G. Whitham. 2017. Tree genetics defines fungal partner communities that may confer drought tolerance. Proceedings of the National Academy of Sciences, U. S. A. 114:11169-11174.

Gifford, E. M. and A. S. Foster. 1989. *Morphology and Evolution of Vascular Plants*, Freeman, NY, NY.

Gould, R. E. 1968. Morphology of *Equisetum laterale* Phillips, 1829, and *E. bryanii sp. nov*. from the Mesozoic of South-Eastern Queensland. Australian Journal of Botany 16:153-176.

Graham, L. E., J. M. Graham, J. J. Knack, M. T. Trest, M. J. Piotrowski, and P. Arancibia-Avila. 2017. A sub-Antarctic peat moss metagenome indicates microbiome resilience to stress and biogeochemical functions of early Paleozoic terrestrial ecosystems. International Journal of Plant Sciences 178:618-628.

Graham, L. E., J. M. Graham, L. W. Wilcox, M. E. Cook, P. Arancibia-Avila, and J. J. Knack. 2018. Evolutionary roots of plant microbiomes and biogeochemical impacts of nonvascular autotroph-microbiome systems over deep time. International Journal of Plant Sciences 179:505-522.

Guerriero, G., C. Law, I. Stokes, K. L. Moore, and C. Exley. 2018. Rough and tough. How does silicic acid protect horsetail from fungal infection? Journal of Trace Elements in Medicine and Biology 47:45-52.

Hartley, A. J., G. Chong, J. Houston, and A. E. Mather. 2005. 150 million years of climatic stability: Evidence from the Atacama Desert, northern Chile. Journal of the Geological Society of London 162:421-424.

Hodson, E., F. Shahid, J. Basinger, and S. Kaminskyi. 2009. Fungal endorhizal associates of *Equisetum* species from Western and Arctic Canada. Mycological Progress 8:19-27.

Hoysted, G. A., A. S. Jacob, J. Kowal, P. Giesemann, M. I Bidartondo, J. G. Duckett, G. Gebauer, W. R. Rimington, S. Schornack, S. Pressel, and K. J. Field. 2019. Mucoromycotina fine root endophyte fungi form nutritional mutualisms with vascular plants. Plant Physiology doi:https//doi.org/10.1104/pp.00729.

Hulse, J. D. 2018. Review of comprehensive staining techniques used to differentiate arbuscular mycorrhizal fungi from plant root tissues. Acta Scientific Agriculture 2.7:39-44.

Husby, C. 2013. Biology and functional ecology of *Equisetum* with emphasis on the giant horsetails. Botanical Review 79:147-177.

Husby, C., J. Delatorre, V. Oreste, S. F. Oberbauer, D. T. Palow, L. Novara, and A. Grau. 2011. Salinity tolerance ecophysiology of *Equisetum giganteum* in South America: a study of 11 sites providing a natural gradient of salinity stress. AoB Plants plr022 doi:10.1093/aobpla/plr022.

Husby, C. E., J. Delatorre-Herrera, S. F. Oberbauer, A. Grau, and L. Novara. 2014. Stomatal conductance patterns of *Equisetum giganteum* stems in response to environmental factors in South America. Botany 92:701-712.

Ionescu, D., C. Siebert, L. Polerecky, Y. Y. Munwes, C. Lott, S. Häusler, M. Bozoc-Ionescu, C. Quast, J. Peplies, F. O. Glöckner, A. Ramette, T. Rödiger, T. Dittmar, A. Oren, S. Geyer, H.-J. Stärk, M. Sauter, T. Licha, J. B. Laronne, and D. de Beer. 2012. Microbial and chemical characterization of underwater fresh water springs in the Dead Sea. Public Library of Science One 7:e38319.

Katoh, K. and D. M. Standley. 2013. MAFFT multiple sequence alignment software version 7: improvements in performance and usability. Molecular Biology and Evolution 30:772-780.

Klindworth, A., E. Pruesse, T. Schweer, J. Peplies, C. Quast, M. Horn, and F. O. Glöckner. 2013. Evaluation of general 16S ribosomal RNA gene PCR primers for classical and next-generation sequencing-based diversity studies. Nucleic Acids Research 41:e1.

Knack, J. J., L. W. Wilcox, P.-M. Delaux, J.-M. Ané, M. J. Piotrowski, M. E. Cook, J. M. Graham, and L. E. Graham. 2015. Microbiomes of streptophyte algae and bryophytes suggest that a functional suite of microbiota fostered plant colonization of land. International Journal of Plant Sciences 176:405-420.

Knief, C., R. Bol, W. Amelung, S. Kusch, K. Frindte, E. Eckmeier, A. Jaeschke, T. Dunai, B. Fuentes, R. Mörchen, T. Schütte, A. Lücke, E. Klumpp, K. Kaiser, and J. Rethemeyer. 2020. Tracing elevational changes in microbial life and organic carbon sources in soils of the Atacama Desert. Global and Planetary Change 184:103078.

Koske, R. E., C. F. Friese, P. D. Olexia, and R. L. Hauke. 1985. Vesicular-arbuscular mycorrhizas in *Equisetum*. Transactions of the British Mycological Society 85:350-353.

Kowal, J., S. Pressel, J. G. Duckett, M. I. Bidartondo, and K. J. Field. 2018. From rhizoids to roots. Experimental evidence of mutualism between liverworts and ascomycete fungi. Annals of Botany 121:221-227.

Laenen, B., B. Shaw, H. Schneider, B. Goffinet, E. Paradis, A. Désamoré, J. Heinrichs, J. C. Villarreal, S. R. Gradstein, S. F. McDaniel, D. G. Long, L. L. Forrest, M. L. Hollingsworth, B. Crandall-Stotler, E. C. Davis, J. Engel, M. Von Konrat, E. D. Cooper, J. Patiño, C. J. Cox, A. Vanderpoorten, and A. J. Shaw. 2014. Extant diversity of bryophytes emerged from post-Mesozoic diversification bursts. Nature Communications 5:5134.

Li, D., C. M. Liu, K. Sadakane, and T. W. Lam. 2015. MEGAHIT: an ultra-fast single-node solution for large and complex metagenomics assembly via succinct de Bruijn graph. Bioinformatics 15:1674-1676.

Li, H. and R. Durbin. 2009. Fast and accurate short read alignment with Burrows-Wheeler transform. Bioinformatics 25:1754-1760.

Li, H., B. Handsaker, A. Wysoker, T. Fennell, J. Ruan, N. Homer, G. Marth, G. Abecasis, and R. Durbin. 2009. 1000 genome project data processing subgroup, the sequence alignment/map format and SAMtools. Bioinformatics 25:2078-2079.

Li, W. and A. Godzik. 2006. Cd-hit: a fast program for clustering and comparing large sets of protein or nucleotide sequences. Bioinformatics 22:1658-1659.

Miller, M. A., W. Pfeiffer and T. Schwartz. 2010. Creating the CIPRES Science Gateway for inference of large phylogenetic trees. In 2010 gateway computing environments workshop (GCE), leee pp.1-8.

Nopun, P., P. Traiperm, T. Boonkerd, and T. Jenjettikul. 2016. Systematic importance of rhizome stellar anatomy in selected Monilophytes from Thailand. Taiwania 61:175-184.

Nouhra, E., C. Urcelay, S. Longo, and L. Tedersoo. 2013. Ectomycorrhizal fungal communities associated to *Nothofagus* species in northern Patagonia. Mycorrhiza 23:487-496.

Ogura-Tsujita, Y., K. Yamamoto, Y. Hirayama, A. Ebihara, N. Morita, and R. Imaichi. 2019. Fern gametophytes of *Angiopteris lygodiifolia* and *Osmunda japonica* harbor diverse Mucoromycotina fungi. Journal of Plant Research 132:581-588.

Ondov, B., N. Bergman, and A. Phillippy. 2011. Interactive metagenomic visualization in a web browser. BMC Bioinformatics 12:385.

Ortega, C., G. Vargas, M. Rojas, J. A. Rutlant, P. Muñoz, C. B. Lange, S. Pantoja, L. Dezileu, and L. Ortlieb. 2019. Extreme ENSO-driven torrential rainfalls at the southern edge of the Atacama Desert during the Late Holocene and their projection into the 21st century. Global Planetary Change https://doi.org/10, 1016/j.gloplacha. 2019.02.011.

Placzek, C., D. E. Granger, A. Matmon, J. Quade, and U. Ryb. 2014. Geomorphic process rates in the Central Atacama Desert, Chile: Insights from cosmogenic nuclides and implications for the onset of hyperaridity. American Journal of Science 314:1462-1512.

Powell, M. J. 2017. Chytridiomycota. Pp. 1523-1558, *in:* J. M. Archibald, A. G. B. Simpson, C. H. Slamovits, L. Margulis, M. Melkonian, D. J. Chapman, and J. O. Corliss (eds), *Handbook of the Protists*. Springer, New York.

Pruesse, E., J. Peplies, and F. O. Glöckner. 2012. SINA: accurate high throughput multiple sequence alignment of ribosomal rna genes. Bioinformatics doi:10.1093/bioinformatics/bts252.

Quast, C., E. Pruesse, P. Yilmaz, J. Gerken, T. Schweer, P. Yarza, J. Peplies, and F. O. Glöckner. 2013. The SILVA ribosomal RNA gene database project: improved data processing and web-based tools. Nucleic Acids Research 41:D590-D596.

Quinlan, A. R. and I. M. Hall. 2010. BEDTools: a flexible suite of utilities for comparing genomic features. Bioinformatics 26: 841-842.

Ragonezi, C. and M. A. Zavattieri. 2018. Histological studies of mycorrhized roots and mycorrhizal-like-structures in pine roots. Methods and Protocols 1:34.

Read, D. J., J. G. Duckett, R. Francis, R. Ligrone, and A. Russell. 2000. Symbiotic fungal associations in 'lower' land plants. Philosophical Transactions of the Royal Society of London B 355:815-831.

Rocha, J. R. S., N. D. C. Sousa, M. A. M. Macedo, L. W. Saraiva, L. A. Santos, A. L. M. Sousa, P. C. L. Sales, A. A. Cronemberger, A. S. Gomes, E. P. Rodrigues, L. M. A. Sousa, and D. F. M. Silva. 2015. First records of *Monoblepharella taylori* Sparrow (Monoblepharidales) in Brazil. Current Research in Environmental and Applied Mycology 5:74-77.

Ronquist, F. and J. P. Huelsenbeck. 2003. MrBayes 3: Bayesian phylogenetic inference under mixed models. Bioinformatics 19:1572-1574.

Rothwell, G. W. 1996. Pteridophytic evolution: An often underappreciated phytological success story. Review of Palaeobotany and Palynology 90:209-222.

Rothwell, G. W. and S. R. Ash. 2015 Internal anatomy of the Late Triassic *Equisetocaulis gen. nov.*, and evolution of modern horsetails. Journal of the Torrey Botanical Society 142:27-37.

Rubinstein, C. V., E. Petus, and H. Niemeyer. 2017. Palynostratigraphy of the Zorritas Formation, Antofagasta region, Chile: Insights on the Devonian/Carboniferous boundary in western Gondwana. Geoscience Frontiers 8:493-506.

Smant, G., J. Helder, and A. Goverse. 2018. Parallel adaptations and common host cell responses enabling feeding of obligate and facultative plant parasitic nematodes. Plant Journal 93:686-702.

Spatafora, J. W., Y. Chang, G. L. Benny, K. Lazarus, M. E. Smith, M. L. Berbee, G. Bonito, N. Corradi, I. Grigoriev, A. Gryganskyi, T. Y. James, K. O'Donnell, R. W. Roberson, T. N. Taylor, J. Uehling, R. Vilgalys, M. M. White, and J. E. Stajich. 2016. A phylum-level phylogenetic classification of zygomycete fungi based on genome-scale data. Mycologia 108:1028-1046.

Stamatakis, A. 2014. RAxML version 8: a tool for phylogenetic analysis and post-analysis of large phylogenies. Bioinformatics 30:1312-1313.

Stringlis, I. A., K. Yu, K. Feussner, R. de Jonge, S. Van Bentum, M. C. Van Verk, R. L. Berendsen, P. A. H. M. Bakker, I. Feussner, and C. M. J. Pieterse. 2018. MYB72-dependent coumarin exudation shapes root microbiome assembly to promote plant health. Proceedings of the National Academy of Sciences, U. S. A. 115:E5213-E5222.

Tedersoo, L., K. Hansen, B. A. Perry, and R. Kjoller. 2006. Molecular and morphological diversity of pezizalean ectomycorrhizal. New Phytologist 170:581-596.

Tedersoo, L., S. Sanchez-Ramirez, U. Koljalg, M. Bahram, M. Doring, D. Schigel, T. May, M. Ryberg, and K. Abarenkov. 2018. Hi-level classification of the Fungi and a tool for evolutionary ecological analyses. Fungal Diversity 90:135-159.

Tipke, I., L. Bucker, J. Middelstaedt, P. Winterhalter, M. Lubienski, and T. Beuerle. 2019. HILIC HPLC-ESI-MS/MS identification and quantification of the alkaloids from the genus *Equisetum*. Phytochemical Analysis 2019:1-10.

Tubaki, K. 1956. *Cephaliophora irregularis* newly found in Japan. Journal of Japanese Botany 31:161-164.

VANNESTE, K., L. STERCK, A. A. MYBURG, Y. VAN DE PEER, and E. MIZRACHI. 2015. Horsetails are ancient polyploids: Evidence from *Equisetum giganteum*. Plant Cell 27:1567-1578.

VOIGHT, C., S, KLIPSCH, D, HERWARTZ, G. CHONG, and M. STAUBWASSER. 2020. The spatial distribution of soluble salts in the surface soil of the Atacama Desert and their relationship to hyperaridity. Global and Planetary Change 184:103077.

WALTERS, W. A., Z. JIN, N. YOUNGBLUT, J. G. WALLACE, J. SUTTER, W. ZHANG, A. GONZÁLEZ-PEÑA, J. PEIFFER, O. KOREN, Q. SHI, R. KNIGHT, S. G. TRINGE, E. S. BUCKLER, J. L. DANGL, and R. E. LEY. 2018. Large-scale replicated field study of maize rhizosphere identifies heritable microbes. Proceedings of the National Academy of Sciences, U. S. A. 115:7368-7373.

WHITE, D. 1894. Equiseta in the Carboniferous. Botanical Gazette 19:71.

WU, G.-L., T.-H. KUO, T.-T. TSAY, I. J. TSAI, and P. J. CHEN. 2016. Glycoside hydrolase (GH) 45 and 5 candidate cellulases in *Aphelenchoides besseyi* isolated from bird's-nest fern. Public Library of Science One 11:e0158663.

YEOH, Y. K., P. G. DENNIS, C. PAUNGFOO-LONHIENNE, L. WEBER, R. BRACKIN, M. A. RAGAN, S. SCHMIDT, and P. HUGENHOLTZ. 2017. Evolutionary conservation of a core root microbiome across plant phyla along a tropical soil chronosequence. Nature Communications 8:215.

ZHANG, L., C. J. LILLEY, M. IMREN, J. P. KNOX, and P. E. URWIN. 2017. The complex cell wall composition of syncytia induced by plant parasitic cyst nematodes reflects both function and host plant. Frontiers in Plant Science 8:1087.

ZHANG, W.-W., C. WANG, R. XUE, and L.-J. WANG. 2019. Effects of salinity on the soil microbial community and soil fertility. Journal of Integrative Agriculture 18:1360-1368.

APPENDIX 1. Ecological and geographical metadata for two sampled Atacama Desert locations.

	Huasqueña (HUA)	**Chiza (CHI)**
Sampling date	1/9/2016	1/10/2016
GPS coordinates	-19.752535 -69.404068	-19.198696 -70.043582
Temperature	31°C	30°C
Altitude	1983 m	350 m
Additional locale information	Remote roadside stream bed; ~0.3 m of dry sedge debris over soil; dry to 20 cm depth, then moist	Chiza valley ~100 m from Chilean highway 5; sandy upper banks of stream bed
Rhizome depth in soil	~0.3 m	>1 m; not collected
Root depth in soil	~0.3 m	~0.3 m

APPENDIX 2. Shotgun Metagenomic Assembly Statistics and Chimera Detection

Site	**HUA**	**CHI**
Number final contigs	432,156	256,891
Minimum contig length, bp	200	362
Maximum contig length, bp	811,711	294,792
Average contig length, bp	362	637
N50, bp	622	664
Number of non-chimeric sequences	SSU 156 LSU 14,231	SSU 113 LSU 11,308
Number of chimeric sequences	SSU 14 LSU 0	SSU 24 LSU 0

APPENDIX 3. SILVAngs Classification Project information: SSU (18S + 16S rDNA) and LSU (23S + 28S rDNA) for sites HUA and CHI, SINA v1.2.10 for ARB SVN (revision 21008)

	SSU HUA	LSU HUA	SSU CHI	LSU CHI
Number samples	1	1	1	1
Number of assembled contigs	432,156	432,156	256,891	256,891
Number of rejected contigs	431,979 (99.96%)	417,906 (96.7%)	256,747 (99.94%)	245,524 (95.58%)
Raw sequence information				
Minimum length	200	200	200	200
Average length	632	632	637	637
Maximum length	811,711	811,711	294,792	294,792
Aligned sequence information				
Minimum length	1	1	1	1
Average length	598	623	589	625
Maximum length	811,711	811,711	294,792	294,792
Quality information: rejected by				
Alignment BP score	39	2951	23	1587
Alignment identity	351018	317010	240132	213804
Alignment score	1528	20884	1244	16601
Ambiguous bases	-	-	-	-
Homopolymers	72978	72693	10652	10481
Quality	-	-	-	-
Length	6416	4368	4696	3051
Clustering information				
Number OTUs	170	14,231	137	11,308
Number clustered sequences	4	18	4	57
Number replicates	3	1	3	2
Classification information				
Number classified sequences	87	185	106	135
Number No-relative	79	14,046	7	11,173
Project settings				
Minimum alignment identity	50	40	50	40
Minimum alignment score	40	30	40	30
Minimum basepair score	30	30	30	30
Quality control				
Minimum sequence quality	30	30	30	30
Minimum length aligned nucleotides	50	50	50	50
Maximum ambiguities (%)	2	2	2	2
Maximum homopolymers (%)	2	2	2	2
Clustering				
CD-Hit Version	3.1.2	3.1.2	3.1.2	3.1.2
Minimum OTU identity	98	98	98	98
Classification				
BLAST version	2.2.30+	2.2.30+	2.2.30+	2.2.30+
Reference	SILVA	SILVA	SILVA	SILVA
Reference version	132	132	132	132
Similarity %	93	93	93	93